CRACK WIDTHS IN CONCRETE WITH FIBERS AND MAIN REINFORCEMENT

Frede Avnskov Christensen, Jens Peder Ulfkjær & Rune Brincker.

Aarhus University, Department of Engineering, DK-8000 Aarhus C, Denmark

Abstract

The main object of the research work presented in this paper is to establish design tools for concrete structures where main reinforcement is combined with addition of short discrete steel fibers. The work is concerned with calculating and measuring crack widths in structural elements subjected to bending load. Thus, the aim of the work is to enable engineers to calculate crack widths for flexural concrete members and analyze how different combinations of amounts of fibers and amounts of main reinforcement can meet a given maximum crack width requirement. A mathematical model including the ductility of the fiber reinforced concrete (FRC) is set up and experimental work is conducted in order to verify the crack width model. The ductility of the FRC is taken into account by using the stress crack width relation. The constitutive model for the FRC is based on the idea that the initial part of the stress crack width relation can be described by a linear relation between load and crack width, taking into account the stresses caused by aggregate interlocking. The second part of the stress crack width relation is described by constant stresses from the fiber bridging stresses. The main idea of the analytical model is to assume that the response of the structure can be described by the cracking response located within a fracture band. The model follows ideas previously used by other researchers in order to describe the fracture mechanics of concrete beams. These ideas are extended in this model to take into account the fiber reinforcement and the pullout of the main reinforcement. By applying suitable kinematics conditions for the fracture band, the deformations within the fracture band correspond to a crack width profile where the crack width varies along the depth of the beam. The stress crack width relation is taken into account according to the crack width profile. Pullout of the main reinforcement is taken into account by assuming development of zones around the crack with constant friction stresses. In order to evaluate the capability of the model to produce reliable results, results are compared with results from experimental investigations.

Keywords: Steel fibres

1 Introduction

After the introduction of the fictitious crack model (Hillerborg, Modeer & Petersson 1976) a lot of attention has been devouted on how this model can be applied to describe the fracture of concrete. The idea of a crack band model was first proposed by Bazant and Oh (Bazant & Oh 1983). Bosco and Carpinteri (Bosco & Carpinteri 1990) were the first to apply these ideas on an analytical model for the minimum requirements of concrete structures. To model size effects in plain concrete beams Ulfkjær, Krenk and Bricker (Ulfkjær, Krenk & Brincker 1995) developed a fracture band model. In this work the fracture band model assumed a linear softening relation for the concrete. Planas, Guinea and Elices (Planas, Guinea & Elices 1995) used a model, based on the same ideas, with a linear softening relation in order to describe aspects concerning the modulus of rupture of plain concrete beams and used these considerations to investigate the minimum reinforcement requirements for reinforced concrete beams. In connection with a work on ligthly reinforced high strength concrete, Hededahl and Kroon (Hededahl & Kroon 1991) derived a fracture band model with main reinforcement. They used a linear softening relation for the concrete and assumed perfect bond between concrete and main reinforcement.

The model presented here extend the previous work in two ways. A stress crack width relation suitable for describing FRC is used and pullout of the main reinforcement is taken into account. It should be noticed that a simmilar work has been performed by Olesen (Olesen 2001), however in this work another constitutive model has been adopted for the FRC and the developement of the zones with constant friction stresses is done in another way than in the work presented here.

2 Model

In this section the analytical model is established. The main assumptions are divided into two sections; one dealing with assumptions concerning the stress-strain relation of the fracture band and one section dealing with the pullout of the main reinforcement.

2.1 Stress strain relation for FRC

Exposing a plain concrete specimen to uniaxial tension, linear proportionality between the load and the deformations are usually a valid assumption for small values of the load. At this stage the deformations are uniformly distributed along the specimen. Performing the tensile loading by monotonously increasing the deformation of the specimen, a peak load occurs when the tensile strength is reached. After the peak load is reached, the deformations are localized due to formation of a crack. For this crack to open pullout of the aggregate from the cement paste will occur leading to a tensile stress σ being transferred through the crack. Increasing the crack width leads to smaller values of the load transferred through the crack. It has previously been shown that this initial part of the stress crack width relation can be described by a linear relation, fig. 1, See e.g. (Elices, Guinea & Planas 1994), (Jensen 2002) and (Brincker, Simonsen & Hansen 1997). A selection of different methods for characterizing the flexural toughness of fiber reinforced concretes can be found in e.g. (Li, Stang & Krenchel 1993), (Simonsen 2001), (ACI 1988), (ASTM C1018 1992), (EFNARC), (IBN 1992), (JCI 1984), (NB 1993), (RILEM 1984), (Henegar 1978) and (Gopalaratnam & Gettu 1995). In FRC slip between the concrete and the fibers is necessary for the crack to open. The fibers crossing the cracked cross section are transferring tensile stress through the crack (here denoted the fiber brigding stresses), thus increasing the resistance for the crack to open. Pullout of the fibers need to take place before the maximum value of the fiber brigding stress occurs, thus for small crack widths the transferred stress can be contributed to the concrete aggregate interlocking and for larger crack widths the stress transfer is caused by the fibers. For most practical purposes the length of the fibers are large compared to the crack widths that are acceptable in concrete structures, leading to a rather small slope on the stress crack width relation from the fiber brigding stresses. It is therefore reasonable to assume constant stresses transferred by the fibers for the crack widths relevant for practical applications. In order to describe the initial part of the stress crack width relation, the tensile strength f_t and the crack width w_1 is introduced. To describe the constant fiber brigding stresses, the parameter γ is introduced, fig. 1.
To be able to translate the stress crack width relation into a stress strain relation, a fracture band is introduced. The fracture band is assumed to deform in such a way that the sections remain plane. Following this approach the crack opening w is smeared through the thickness of the fracture band with length h.

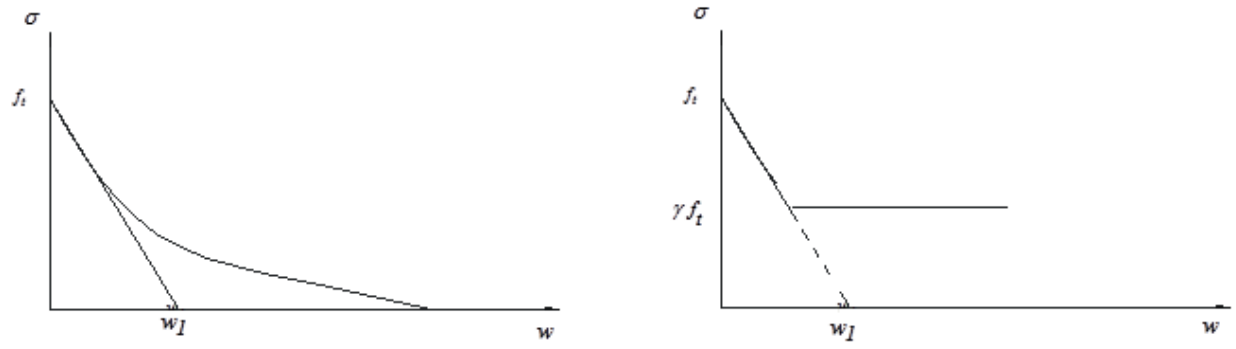

Fig. 1 *Stress crack width relation for FRC.*

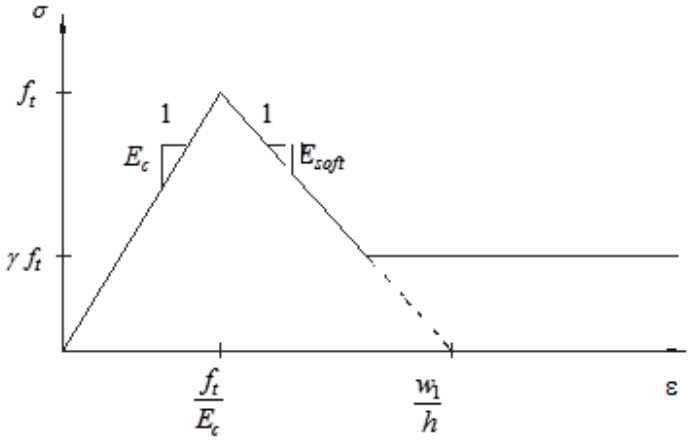

Fig. 2 *Stress strain relation of the fracture band.*

The deformations within the fracture band consist partly of the crack width and elastic deformations, fig. 2. Thus the strain within the fracture band is described by:

$$\varepsilon = \frac{\sigma}{E_c} + \frac{w}{h} \tag{1}$$

Where E_c is the Young modulus of the FRC. The stress strain relation is divided into three parts. A first part with strain less than the critical value f_t/E_c. A second part, in the following to be denoted the softening part of the stress strain relation, where the stress and strain may related through the slope E_{soft} which may be expressed as, fig. 2:

$$E_{soft} = kE_c \qquad \text{where} \qquad k = \frac{h}{l_1 - h} \tag{2}$$

where the characteristic length l_1 is defined by:

$$l_1 = \frac{E_c w_1}{f_t} \tag{3}$$

Increasing the length of the fracture band h increases the value of k and the absolute value of the softening modulus E_{soft}. When $h \rightarrow l_1$ the slope of the softening part becomes vertical. Thus the model is only valid until a certain degree of brittleness of the structure. For the third part of the stress strain relation, the stress is equal to the constant fiber brigding stress γf_t.

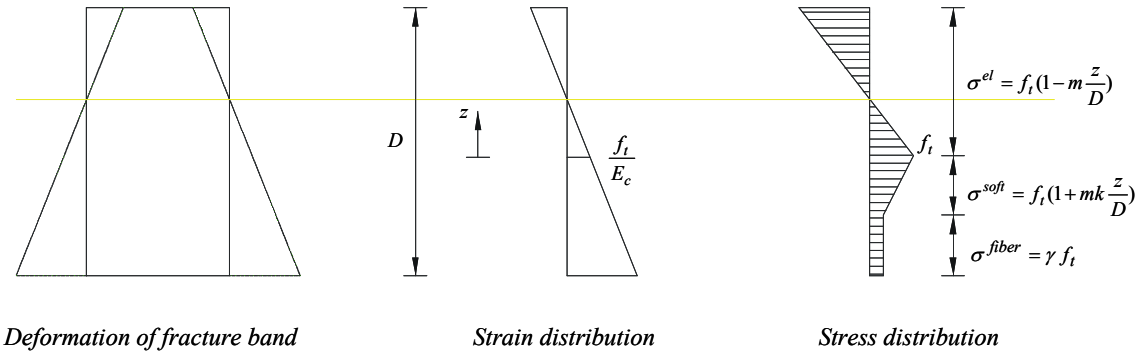

Fig. 3 *Basic assumptions concerning the kinematics of the fracture band and the corresponding stress distribution.*

The kinematic of the fracture band is shown in fig. 3. The z-axis is located with origin at the point of the section where the tensile strength is reached (the positive direction is shown in fig. 3). The strain at any point on the cross section can be written as:

$$\varepsilon = \frac{f_t}{E_c}\left(1 - m\frac{z}{D}\right) \tag{4}$$

where m is a dimensionless number describing the slope of the stress distribution in the uncracked part of the cross section. In order to describe the extension of a crack through the beam depth, it is now assumed that a point on the crack extension path can be in one of 3 possible states: A state where the behaviour is elastic (uncracked part of the cross section), A state where the behaviour is described by the softening relation and a state where the stress is constant. Expressions for the stresses at these different states are given in fig. 3.

2.2 Pull-out of the main reinforcement

The significance of this study is concerned with how to include the main reinforcement. Before the crack crosses the main reinforcement, perfect bond between the steel and the concrete is assumed. In order for the crack to open, slip between the steel and the concrete has to occur. In this model this is taken into account by assuming developement of zones around the crack with constant friction stresses. Consider the situation around the main reinforcement shown in fig. 4. The stress in the steel at the crack face is equal to σ_s. At the crack faces the stress σ_c is acting. A zone of constant friction stresses equal to τ_c with the length l_d is developed at each side of the crack. Now assuming that the stress at the end face of the debonded zone is equal to σ_c the relation betweeen the length l_d and the crack width w_s is given by integrating the differences in strain between the steel and the concrete:

$$l_d = \sqrt{\frac{E_s r_d}{2\tau_c} w_s} \tag{5}$$

Where E_s is the Young modulus for the main reinforcement and r_d is the radius of the rebars. Considering equvilibrium of the reinforcement alone one gets:

$$\sigma_s = \sqrt{\frac{2\tau_c E_s}{r_d} w_s} + \alpha\sigma_c \tag{6}$$

Where α is E_s/E_c. As can be seen from this equation the relation between the steel stress and the crack width can be divided into two stages. The first stage is the stage where σ_c is described by the softening part of the stress strain relation while the second part of the pullout curve is described by the part with constant fiber brigding stresses.

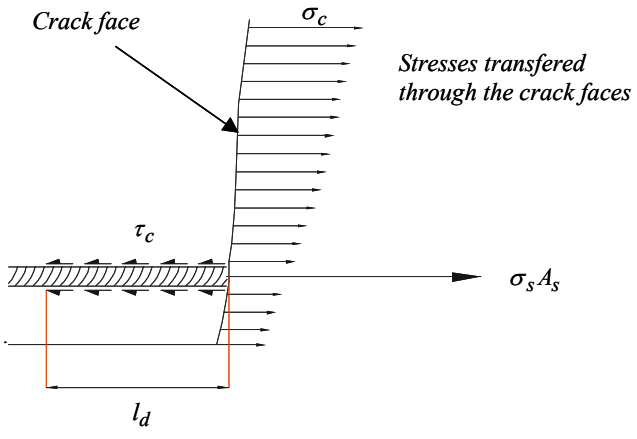

Fig. 4 *Considerations concerning pullout of the main reinforcement*

Introducing the dimensionless steel stress $\sigma_s^* = \sigma_s/f_t$ and the dimensionless crack width $w_s^* = w/w_1$, one gets in dimensionless form:

$$\sigma_s^* = g\sqrt{w_s^*} + \alpha(1 - w_s^*) \qquad \text{and} \qquad \sigma_s^* = g\sqrt{w_s^*} + \alpha\gamma \tag{7}$$

Where g is a dimensionless number describing the bond properties and given by:

$$g = \sqrt{4\frac{\tau_c}{f_t}\frac{l_1}{r_d}\alpha} \tag{8}$$

2.3 Model formulation

The model is established by introducing a number of stages depending on the length of the crack. The equations of the model are set up by analysis of the stress distributions according to these different stages. In the following x denotes the crack length while r denotes the relative crack length x/D. β denotes the cover layer while c denotes the relative cover layer (β/D). The bending moment corresponding to the tensile strength being reached at the bottom of the beam is denoted M_{cr}. The dimensionless load σ is defined by M/M_{cr} where M is the bending moment calculated from the stress distribution.

Stage I is characterized by the crack being below the main reinforcement and that the stresses at the cracked part of the cross section is described by the softening part of the stress strain relation (fig. 5). Perfect bond between the concrete and the steel is assumed, leading to the dimensionless steel stress equal to:

$$\sigma_s^* = \alpha\big(1 + m(r - c)\big) \tag{9}$$

Solving the horizontal equvilibrium equation with respect to the relative crack length r the dimensionless load is found by:

$$\sigma = 6\alpha\rho\sigma_s^*(r - c) - 2kmr^3 + 2m(1 - r)^3 + 6r - 3 \tag{10}$$

Where ρ is the main reinforcement ratio. This stage is valid until the relative crack length r is equal to the relative cover layer c or until the concrete stress at the bottom of the beam is equal to γf_t.

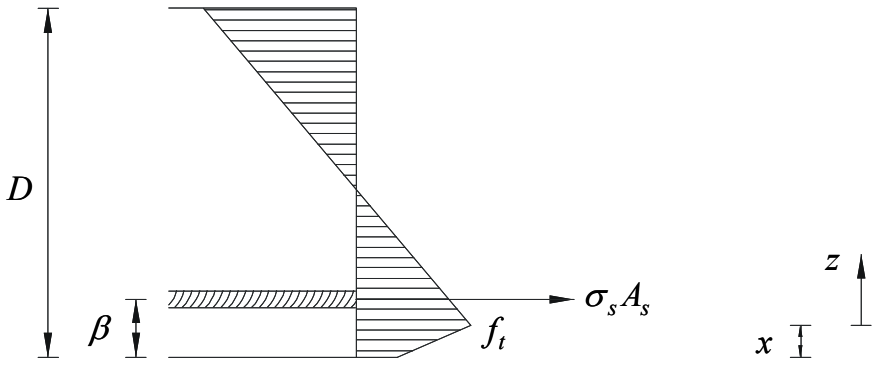

Fig. 5 *Stress distribution in stage I.*

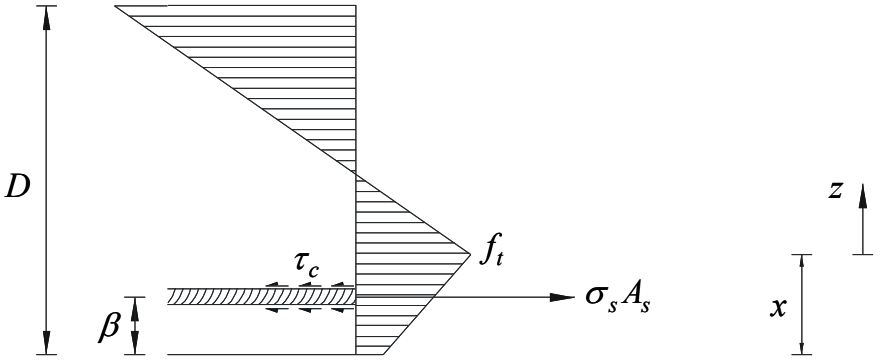

Fig. 6 *Stress distribution in stage IIa.*

In Stage IIa the crack has crossed the main reinforcement and pullout of the reinforcement is starting. Furthermore the stresses in the cracked part of the cross section is described by the the softening curve (fig. 6). Solving the horizontal equvilibrium equation with respect to the relative crack length *r* the dimensionless load is found by:

$$\sigma = 6\sigma_s^*\rho(r-c) + \frac{2w_s^*\left[(1-r)^3 - kr^3\right]}{k(r-c)} + 6r - 3 \tag{11}$$

This stage is valid until the concrete stress at the bottom of the beam is equal to γf_t.

At *stage IIb* a zone with constant stresses is developed at the bottom of the beam before the crack reaches the main reinforcement (fig. 7). Solving the horizontal equvilibrium equation with respect to the relative crack length *r* the dimensionless load is found by:

$$\sigma = 6\alpha\rho\sigma_s^*(r-c) - 3(1-\gamma)r^2 + 2m(1-r)^3 + \frac{(1-\gamma)^3}{m^2k^2} + 6r - 3 \tag{12}$$

This stage is valid until the relative crack length is equal to the relative cover layer.

Stage III is characterized by the crack having crossed the main reinforcement and the stresses in the cracked part of the cross section is partly described by the softening curve and a zone has developed where the stresses are constant. However the zone with constant stresses have not yet crossed the reinforcement (fig. 8). Solving the horizontal equvilibrium equation with respect to the relative crack length *r* the dimensionless load is found:

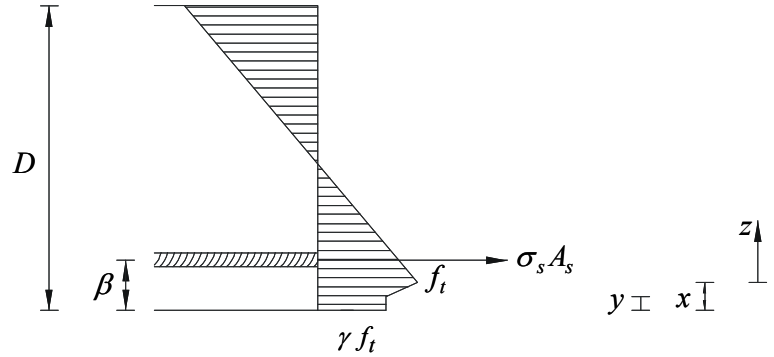

Fig. 7 *Stress distribution in stage IIb.*

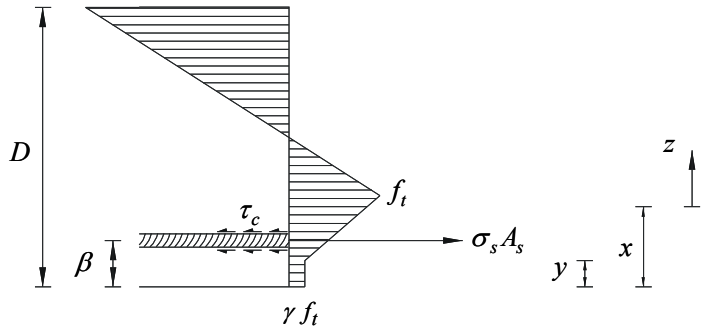

Fig. 8 *Stress distribution in stage III.*

$$\sigma = 6\sigma_s^* \rho(r-c) + \frac{2w_s^*(1-r)^3}{k(r-c)} - 3(1-\gamma)r^2 + \frac{(1-\gamma)^3(r-c)^2}{w_s^{*2}} + 6r - 3 \tag{13}$$

This stage is valid until the zone with constant stresses reaches the reinforcement.

The stress distribution at *stage IV* is shown in fig. 9. Compared with stage III, the pullout curve has changed because the zone with constant stresses has crossed the reinforcement. Introducing ξ by:

$$\xi = (1+k)w_s^* - k(1-\gamma) \tag{14}$$

Solving the horizontal equvilibrium equation with respect to the relative crack length *r* the dimensionless load is found:

$$\sigma = 6\sigma_s^* \rho(r-c) + \frac{2\xi(1-r)^3}{k(r-c)} - 3(1-\gamma)r^2 + \frac{(1-\gamma)^3(r-c)^2}{\xi^2} + 6r - 3 \tag{15}$$

This stage is valid until yielding of the reinforcement occurs.

3 Experiments

In order to evaluate how addition of fibers influences the crack widths, a series of beam tests have been conducted. A total of 12 beams have been tested in 4-point-bending and crack width measurements have been obtained. In the calculation of the reinforcement ratio, stated below, the total height of the beam has been used.

3.1 Test program and specimens

Two different beam sizes are tested with main reinforcement ratios equal to 0.14% and 0.25%. Both high strength concrete (HSC) and normal strength concrete (NSC) have been tested. The test program involves 8 NSC beams and 4 HSC beams. This test program is conducted with plain beams and with beams with 1.0 VOL% hooked steel fibers (DRAMIX 30/.50) (FRC). 4-point-bending is obtained by applying loads at the third-points of the beam. The main reinforcement consists of a single reinforcing steel bar. The beams were cast in steel molds. The test program is shown in table 1.

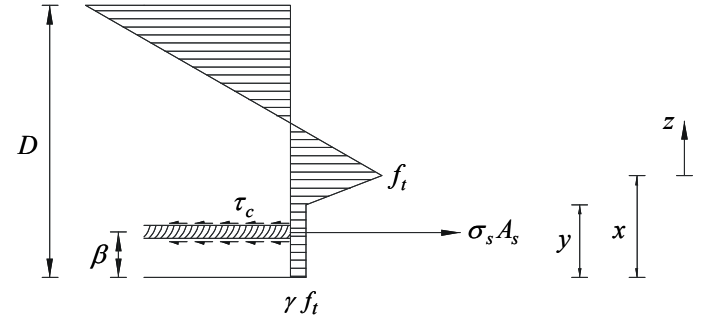

Fig. 9 *Stress distribution in stage IV.*

Beam size	Concrete	Main reinforcement	Reinforcement ratio [%]
100x200x2400 mm	NSC	1 Ø6 mm	0.14
		1 Ø8 mm	0.25
	HSC	1 Ø6 mm	0.14
		1 Ø8 mm	0.25
200x400x4800 mm	NSC	1 Ø12 mm	0.14
		1 Ø16 mm	0.25

Table 1 *Test program for the beam tests. These tests are conducted for a series with no fibers and a series with 1.0 VOL% steel fibers.*

3.2 Material properties

The compression strengths of the concretes were measured on cylinders with a diameter of 100 mm and a length of 200 mm. The loading rate is 6.4 kN/sec. The compression strength of the normal strength concrete is approximately 37 MPa in both cases of plain and FRC beams. In the case of the high strength concrete the compression strength is approximately 100 MPa in the case with plain beams and approximately 85 MPa in the case with FRC beams. To characterize the tensile properties of the concretes load deflection curves were obtained for 100x100x800 mm beams with a notch of 50 mm. These tests were conducted according to the RILEM test procedure for determination of the fracture energy RILEM (1985). During testing the midpoint deflection and the applied load are recorded. The measured bending response is compared with model solutions obtained by using the direct substructure method (Brincker & Dahl 1989). Using different values of the parameter in the constitutive model for the concretes and comparing the calculated load deflection curves with the measured response, appropriate values of the modulus of elasticity E_c, the crack width w_1, the tensile strength f_t and the fiber bridging stresses γ can be found. These values can be seen in table 2. The measured load deflection curves and the corresponding results from the direct substructure method are shown in fig. 10 and 11.

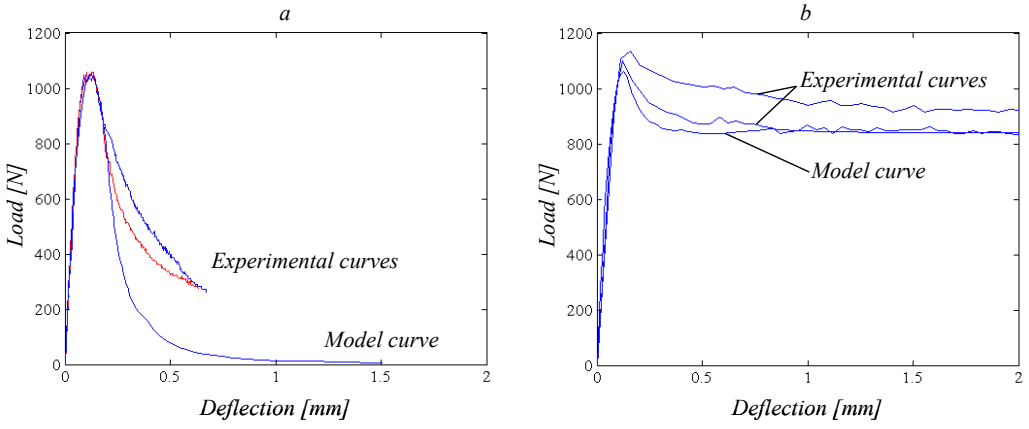

Fig. 10 *Measured and model result for load deflection curves for notched beams of NSC. Left: Concrete without fibers. Right: Concrete with 1.0 VOL% steel fibers.*

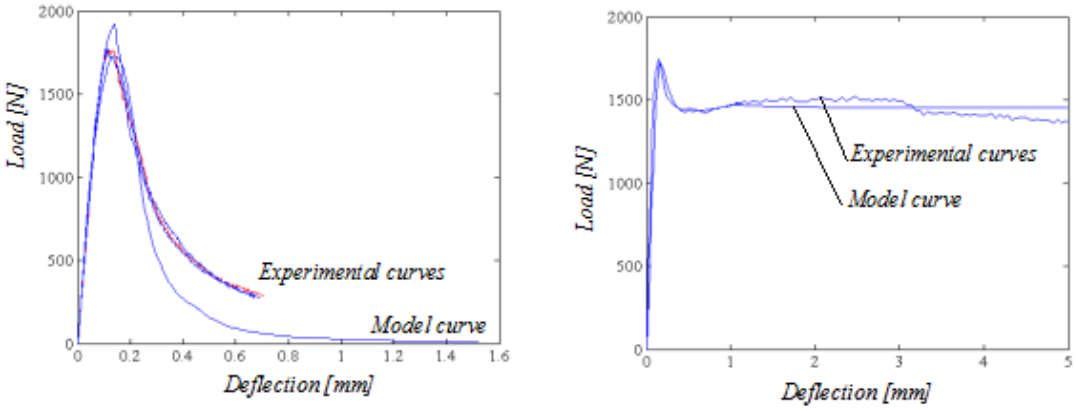

Fig. 11 *Measured and model result for load deflection curves for notched beams of NSC. Left: Concrete without fibers. Right: Concrete with 1.0 VOL% steel fibers.*

Concrete	f_t	E_c	w_1	γ
NSC with no fiber	3.0	20000	0.0367	0.0
NSC with 1.0 VOL% fiber	3.0	20000	0.0367	0.47
HSC with no fiber	5.2	30000	0.0367	0.0
HSC with 1.0 VOL% fiber	5.2	30000	0.0367	0.47

Table 2 *Parameters describing the tensile properties for NSC and HSC.*

In order to get information about the material properties of the main reinforcement, stress strain relations have been measured. From these tests the following parameters were derived; The average value of the modulus of elasticity is approximately 200000 MPa, the yield stress is approximately 550 MPa, the fracture strength is approximately 650 MPa and the fracture strain is approximately 13%. These values are valid for all sizes of main reinforcement used in the beam tests.

3.3 Crack width measurements

In an area around the midsection of the beam, crack width measurements are collected. The test procedure is to load the beam until a certain deflection and crack width measurements are collected while this deflection is fixed. The length of the area of which crack widths are measured is approximately 400 mm. By use of a digital camera the cracks are identified and measured. The camera captures an area of approximately 2x2 mm. The signal from the camera is transferred to a computer screen. This correspond to an enlargement of the image of approximately 100 times, which makes it possible to identify and measure cracks widths that are 0.05 mm. To identify the cracks, the camera is scanning along a line, corresponding to the location of the reinforcement, on the surface of the beam. When a crack is identified, a crack width measurement is performed and an image of the crack is stored on the computer. In fig. 12 three images showing cracks of different widths are shown.

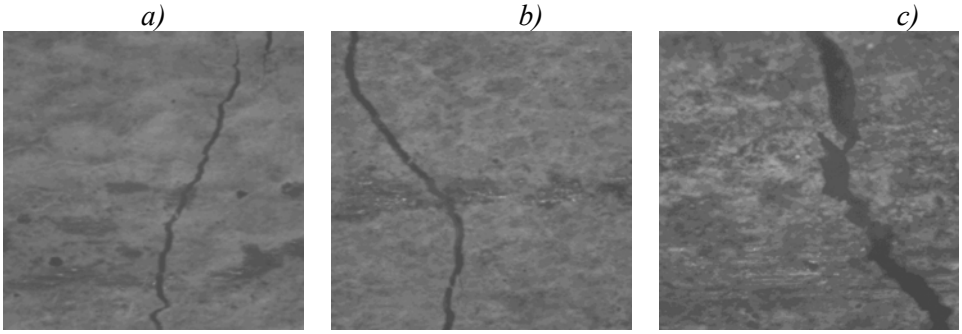

Fig. 12 *Images from crack width measurements. The cracks shown here are measured to a) 0.08 mm. b) 0.12 mm. c) 0.31 mm.*

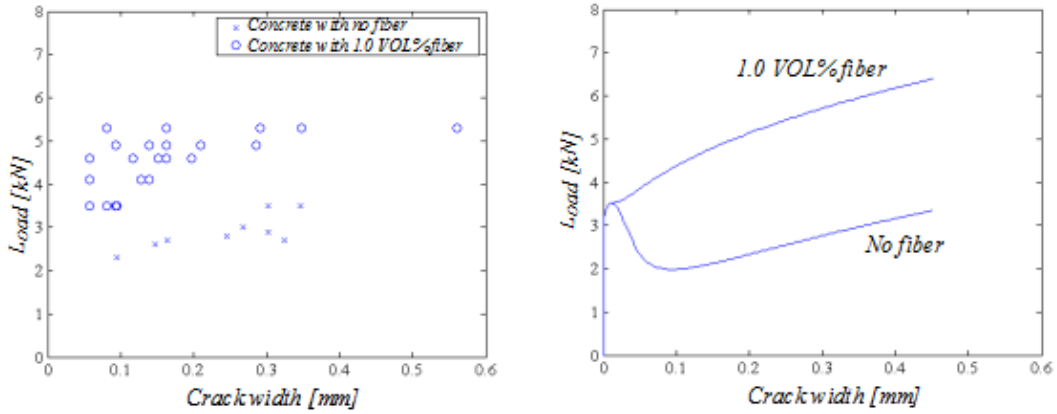

Fig. 13 *Left: crack width measurements for NSC 100x200x2400 mm beam with main reinforcement ratio of 0.14 %. Right: Crack widths obtained from the model.*

4 Comparisons

In this section the crack width measurements are compared with results from the model. In fig. 13 test results and model results are shown for the 100x200x2400 mm NSC beams with main reinforcement of 0.14% . Both the beam tests and the model show a significant influence of the fibers. The model predicts an increase in load after first cracking in the case of the FRC beam, whereas the load decreases after first cracking in the case with no fibers. This is in good agreement with the results from the beam tests. Both model and tests shows a significant increase in the load bearing capacity after cracking in the FRC case. The same tendencies are observed in the case with HSC, fig. 14. In fig. 15 test results and results from the fracture band model are shown for the 100x200x2400 mm NSC beams with main reinforcement of 0.25%. Both the beam tests and the model show a significant influence of the fibers. Also in this case the model predicts an increase in load after first cracking for the FRC beam, whereas the load decreases after first cracking in the case with no fibers. Also here this tendency is confirmed by the test results. Both the model and the beam tests show a significant increase in the load bearing capacity in the case with FRC. Test results and the model shows a reduction of approximately 50% of the crack widths at a load equal to 6 kN although the model predicts slightly larger crack widths, for en given load, than is seen in the beam tests. This is the case for plain concrete as well as for the FRC. In fig. 16 test results and results from the model are shown for the 100x200x2400 mm HSC beams with main reinforcement of 0.25%. The tendencies are the same, however in this case the model overestimates the reduction in crack widths.

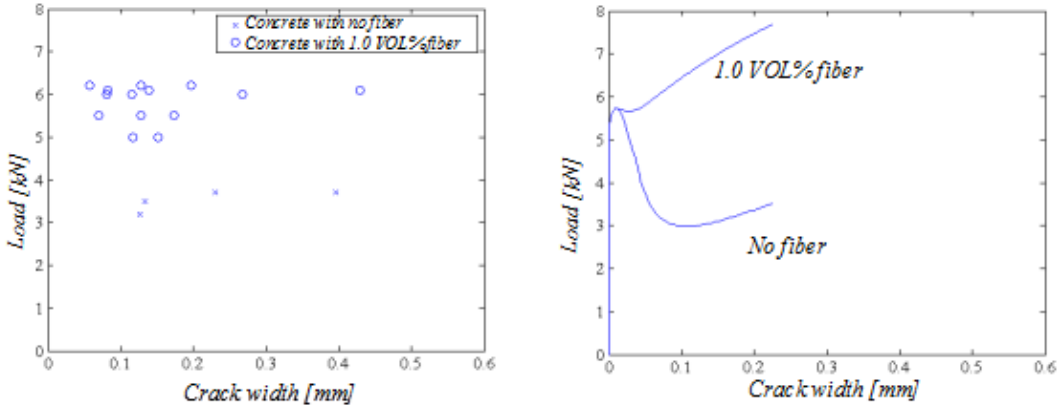

Fig. 14 *Left: crack width measurements for HSC 100x200x2400 mm beam with main reinforcement ratio of 0.14 %. Right: Crack widths obtained from the model.*

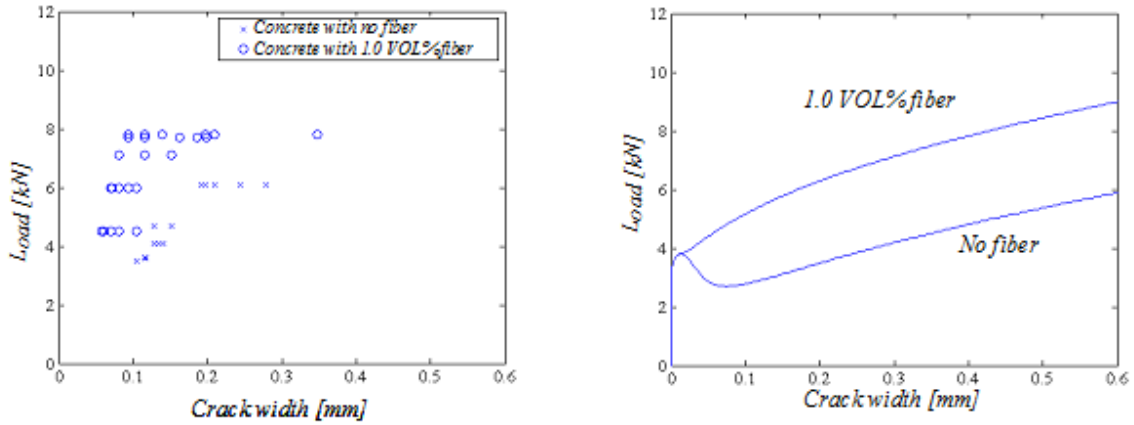

Fig. 15 *Left: crack width measurements for NSC 100x200x2400 mm beam with main reinforcement ratio of 0.25 %. Right: Crack widths obtained from the model.*

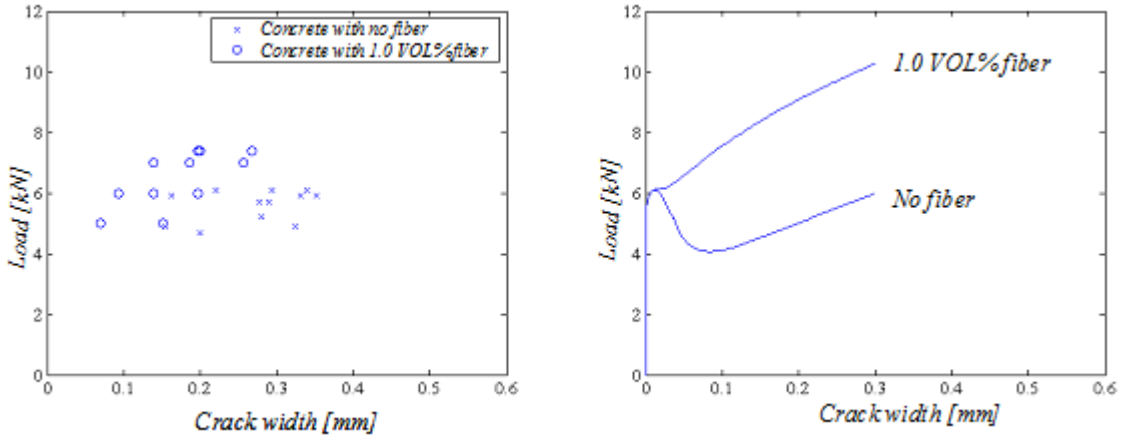

Fig. 16 *Left: crack width measurements for HSC 100x200x2400 mm beam with main reinforcement ratio of 0.25 %. Right: Crack widths obtained from the model.*

Fig. 17and 18 shows results from the 200x400x4800 mm beam. In fig. 17 test results and results from the model are shown for the main reinforcement equal to 0.14% and cast of normal strength concrete. Both the beam tests and the model show a significant influence of the fibers. Both the model and the beam tests show that a reduction of the crack widths of approximately 70% can be obtained by addition of fibers. The beam tests show that in the case of concrete with no fibers, 2 cracks are formed within the measuring area, whereas only 1 crack is formed in the case with fibers. In fig. 18 test results and results from the model are shown for the 200x400x4800 mm beams with main reinforcement of 0.25% and cast of normal strength concrete. At a value of the load equal to 15 kN, the beam tests show that a reduction of the crack widths of approximately 30% by addition of fibers. Also in this case the fracture band model predicts a larger reduction by addition fibers than is observed in the beam tests.

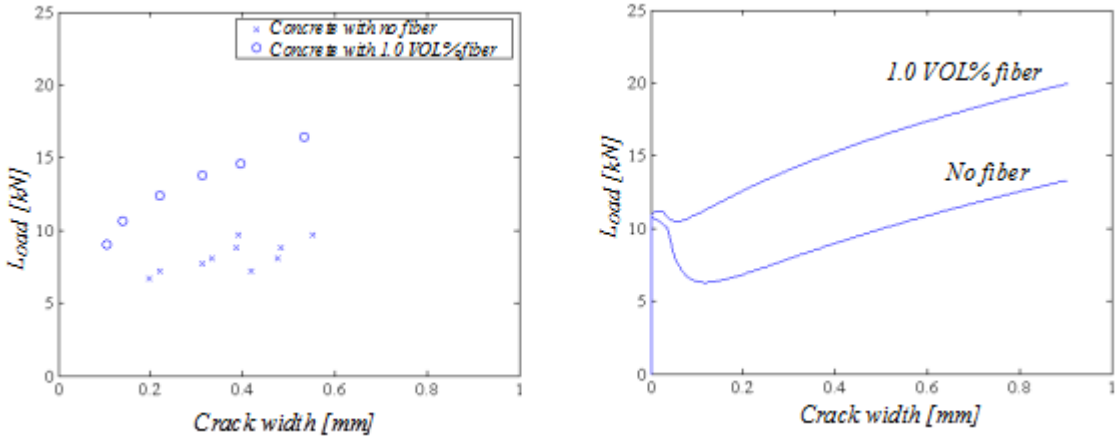

Fig. 17 *Left: crack width measurements for NSC 200x400x4800 mm beam with main reinforcement ratio of 0.14 %. Right: Crack widths obtained from the model.*

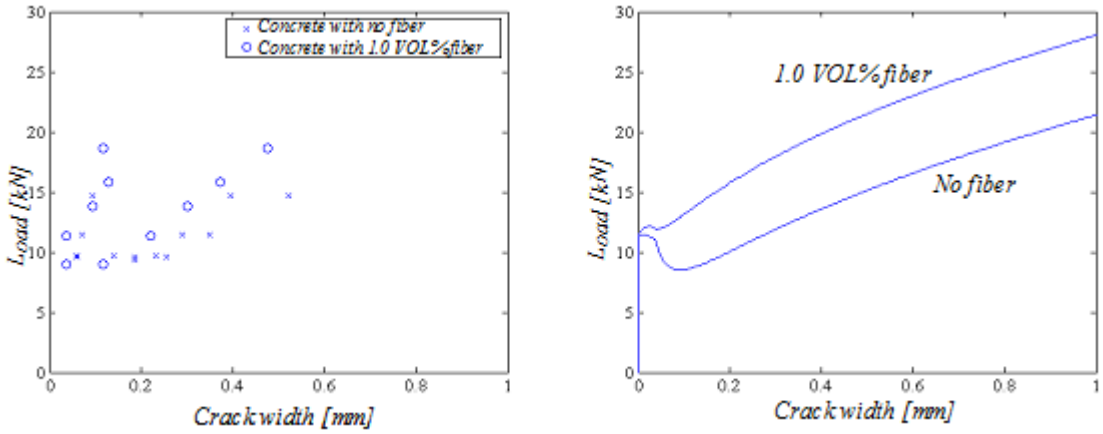

Fig. 18 *Left: crack width measurements for NSC 200x400x4800 mm beam with main reinforcement ratio of 0.25 %. Right: Crack widths obtained from the model.*

5 Conclusions

In this paper a model describing the relation between crack widths and load of a fiber reinforced concrete beam with main reinforcement is established. The main significance of the model is concerned with how to include the main reinforcement. To do this, the slip between the concrete material and the main reinforcement is taken into account by assuming development of zones around the crack with constant friction stresses. According to the model the fracture mechanical behavior of a plain concrete beam can be predicted by the ratio between the beam depth and the characteristic length of the concrete material. In order to include fiber reinforcement the parameter describing the constant fiber bridging stresses is introduced. In order to describe the fracture mechanical behavior of a fiber reinforced beam with main reinforcement, 5 additional parameters are introduced. The model shows that the key parameters in determining crack widths in fiber reinforced concrete structures are the amount of main reinforcement, the bond properties between the concrete material and the main reinforcement, the structure size and the fiber bridging stresses. Generally, the fracture band model predicts an increased effect of addition of fibers for increasing structure size, decreasing amount of main reinforcement and decreasing bond between the concrete material and the main reinforcement. To evaluate the capability of the fracture band model to predict crack widths in fiber reinforced concrete structures, a series of beam tests combining main reinforcement and fibers have been

conducted. These tests have been conducted on beams with varying beam sizes, varying main reinforcement ratios, varying concrete strengths and varying amounts of fibers.

Generally the model shows tendencies that corresponds quite well with the test results. Both the model and the test results shows that unstable crack growth after the first cracking can be avoided by addition of fibes. The model also predicts quite well the significant reduction in crack widths that it is possible to obtain by addition of fibers, althrough the model seems to overestimate the reduction in the case of the main reinforcement ratio equal to 0.25%.

References

ACI (1988), Measurements of properties of fiber reinforced concrete. ACI Mater J. 85(6) (November-December 1988) 583-93.

ASTM C 1018 (1992). Standard Test Method for Flexural Toughness and First-Crack Strength of Fiber-Reinforced Concrete (Using Beam With Third-Point Loading). ASTM, Philadelphia, USA, pp. 510-16.

Bazant Z.P. & Oh. B.H. (1983), Crack Band Theory for Fracture of Concrete, Materials and Structures, 16 1983 pp. 155-177.

Bosco C. & Carpinteri A. (1990), Fracture Mechanics Evaluation of Minimum Reinforcement in Concrete Structures. In Application of Fracture Mechanics to Concrete Structures. Ed. A Carpinteri, Elsevier Applied Science, Italy pp. 347-377.

Brincker R. & Dahl H. (1989), Fictitious Crack Model of Concrete Fracture, Magazine of Concrete Research 41, No. 147 pp 79-86.

Brincker R., Simonsen J. & Hansen W. (1997), Some aspects of formation of cracks in FRC with main reinforcement. In Nordic Concrete Research. Publication no. 20 1997.

EFNARC (1993), Specification for Sprayed Concrete. Final Draft Published by the European Federation of National Associations of Specialist Contractors and Material Suppliers to the Construction Industry (EFNARC). Hampshire. UK, 35 pp.

Elices M., Guinea G.V. & Planas J. (1994). Prediction of Size-effect based on Cohesive Crack Model. In Size-scale effects In the failure mechanisms of materials and structures. Ed. A. Carpinteri. Symposium on Size-scale effects in the failure mechanisms of materials and structures. Torino.

Gopalaratnam V.S. & Gettu R. (1995), On the Characterization of Flexural Toughness in Fiber Reinforced Concretes. In Cement & Concrete Composites 17 pp. 239-254.

Hededahl O. & Kroon I. (1991), Lightly Reinforced High-Strength Concrete. M.Sc. Thesis in Civil Engineering, AUC.

Henegar C.H. (1978), Toughness index of fibre concrete. In Testing and test methods of fibre Cement Composites RILEM Symposium 1978. Construction Press Ltd. Lancaster. UK. Pp 79-86.

Hillerborg, A., Modeer, M & Petersson, P.E. (1976), Analysis of Crack Formation and Crack Growth in Concrete by Means of Fracture Mechanics and Finite Elements, Cement and Concrete Research, pp. 773-782.

IBN (1992). Essais des bétons renforcés de fibres – Essai de flexion sur éprouvettes prismatiques. Norme Belge NBN B 15-238, Institute Belge de Normalisation (IBN), 1040 Brussels, Belgium, 9 pp.

JCI (1984), Method of Tests for Flexural Strength and Flexural Toughness of Fiber Reinforced Concrete, JCI Standard SF-4, Japan Concrete Institute Standards for Test methods of Fiber Reinforced Concrete, Tokyo, Japan, June, pp. 45-51.

Jensen E.A. (2002). Investigation of Cracking Process and Aggregate Interlocking Properties of JPCP Cracks. Ph.D.-thesis at the University of Michigan.

Li V.C., Stang H. & Krenchel H. (1993). Micromechanics of Crack Bridging in Fibre-Reinforced Concrete. Materials and Structures, No. 26.

NB (1993), Sprayed Concrete for Rock Support – Technical Specification and Guidelines. Norwegian Concrete Association (NB, Norsk Betongforening), Publication No. 7, 0251 Oslo, June, 74 pp.

Olesen J.F. (2001), Cracks in reinforced FRC beams subject to bending and axial load. Fourth International Conference on Fracture Mechanics of Concrete and Concrete Structures, Cachan.

Planas J, G.V. Guinea & M. Elices (1995), Rupture modulus and fracture properties of concrete. Fracture Mechanics of Concrete Structures. Ed. F. Wittmann, Germany.

RILEM (1984), Test and Method methods for steel fiber reinforced concrete. Recommendations for uniaxial tension test, Materials and Structures. Prepared by RILEM- Committee- TDF-162.

RILEM (1985). Determination of fracture energy of mortar and concrete by means of three-point bend tests on notched beams. RILEM Draft Recommendation, Mater. Struct. 18(106) 285-90.

Simonsen J. (2001), Fracture Mechanics of Multiple Fibre Systems in Cement-Based Materials. Ph.D-thesis. Department of Building Technology and Structural Engineering, Aalborg University, Denmark.

Ulfkjær J.P., S. Krenk S. & R. Brincker (1995), Analytical model for fictitious crack propagation in concrete beams. Journal of Engineering Mechanics 1995:121(1) pp. 7-14.